Interpretation of XPS Mn(2p) spectra of Mn oxyhydroxides and constraints on the mechanism of MnO_2 precipitation

H.W. Nesbitt and D. Banerjee

Department of Earth Sciences, University of Western Ontario, London, Ontario N6A 5B7, Canada

Abstract

Calculated $Mn(2p_{3/2})$ X-ray photoelectron spectra (XPS) of Mn^{2+}, Mn^{3+}, and Mn^{4+} free ions are strikingly similar to $Mn(2p_{3/2})$ spectra of Mn^{2+}-, Mn^{3+}-, and Mn^{4+}-oxides and oxyhydroxides, indicating that these ions adopt high spin states in MnO, manganite, and birnessite. The Mn(2p) peak structures reveal the presence of only Mn^{3+} in manganite, but Mn^{2+}, Mn^{3+}, and Mn^{4+} are present in the near-surface of synthetic birnessite at about 5, 25, and 70%, respectively. Precipitation of birnessite by reaction of $Mn^{2+}(aq)$ with an oxidant includes two electron transfer steps: (1) oxidation of $Mn^{2+}(aq)$ to produce Mn^{3+}-oxyhydroxide, an intermediate reaction product that forms on the surface of synthetic birnessite and (2) subsequent oxidation of Mn^{3+}-oxyhydroxide surface species to produce synthetic birnessite. Some surface Mn^{3+}, however, remains unoxidized and is incorporated into birnessite. As for this synthesis ($KMnO_4$ used as oxidant), oxidation may not proceed to completion in natural settings (as O_2 is the oxidant) leading to Mn^{3+} incorporation into Mn-oxides. The hypothesis explains the abundance of non-stoichiometric MnO_2 phases in sedimentary environments. The MnO_2 precipitation scheme proposed by Stumm and Morgan (1981) includes the surface species $Mn^{2+} \cdot MnO_2$. This and other studies indicate that the reactive intermediate is a Mn^{3+}-bearing surface species. The formation rate of birnessite is probably controlled by one of these redox reactions. The proposed rate expression of Davies and Morgan (1989), however, needs no modification provided surface area is a reasonable measure of the surface density of the reactive intermediate.

Introduction

Natural Mn-oxides and oxyhydroxides scavenge heavy metals from natural solutions and are important natural and industrial catalysts. Knowledge of the chemical state of elements constituting these phases is therefore of value to industrial chemists and to geochemists. Although numerous studies exist of the products of Mn oxidation (Foord et al. 1984; Di Castro and Polzonetti 1989) we are unaware of any that compare and contrast X-ray photoelectron spectra (XPS) 2p multiplet structures of Mn^{2+}, Mn^{3+}, and Mn^{4+} in oxides and oxyhydroxides or compare them with 2p spectra of other transition metal ions. These aspects are addressed here. Mn(2p) XPS spectra have been of limited value due to difficulties in differentiating among the contributions of Mn^{2+}, Mn^{3+}, and Mn^{4+} to the spectra of most solid Mn phases (Murray et al. 1985). The difficulties are twofold. The peak maxima for the three ions are separated by about two eV, making it difficult to resolve the separate contributions using most instruments; even partial resolution requires peak widths to be less than 1.4 eV the full width at half of maximum (FWHM). Second, Mn^{2+}, Mn^{3+}, and Mn^{4+} generally assume high spin states in oxides and oxyhydroxides (Cotton and Wilkinson 1988), and in high spin states the 2p XPS spectrum of each is composed of numerous peaks (multiplets) that result in unusually broad, compound $Mn(2p_{3/2})$ spectra (Gupta and

Sen 1974, 1975; Kowalczyk et al. 1975; Murray et al. 1985; Junta et al. 1992; Okada and Kotani 1992; Junta and Hochella 1994). Previous XPS studies consequently focused on other spectral lines. The severe difficulties faced by previous investigators were partially surmounted by modified instrumentation and by recent developments in spectral analysis. The focus of this study is the $2p_{3/2}$ XPS spectra of Mn^{2+}, Mn^{3+}, and Mn^{4+} ions of some Mn-bearing oxides and oxyhydroxides, including manganite and synthetic birnessite.

Manceau et al. (1992) used X-ray absorption near edge spectroscopy (XANES) to investigate the chemical state of Mn in hydrous manganese oxides (vernadite, δ-MnO_2, asbolane, and birnessite). Their XANES MnK edge line widths, however, are too broad (near 2 eV) to resolve the three chemical states of Mn. With improvements to the XPS instrument, and use of the maximum entropy methods, our Mn2p line widths are appreciably narrower than MnK edge XANES lines (0.85 eV vs. 2 eV) so that the XPS analysis is much more definitive with regards to chemical states and the abundance of the three oxidation states in solids. XPS analyses reflect, however, only the uppermost few atomic layers of a mineral whereas XANES samples deeper into the bulk.

Junta and Hochella (1994) demonstrated that Mn precipitation on goethite, hematite, and albite proceeded by

oxidation of $Mn^{2+}(aq)$ to Mn^{3+}, which accumulated as an oxyhydroxide surface species. Their findings suggest the possibility that Mn^{3+} surface species are also produced during oxidative precipitation of MnO_2 from $Mn^{2+}(aq)$-bearing solutions. If so, Mn^{3+} surface species may help to explain ambiguities associated with MnO_2 stoichiometry and variation in kinetics of reductive dissolution and oxidative precipitation of Mn oxyhydroxides (Scott and Morgan 1995; Stumm and Morgan 1981). This study provides insight into the nature of substitutions in synthetic birnessite and documents the proportions of Mn^{2+}, Mn^{3+}, and Mn^{4+} in the near-surface of synthetic birnessite.

Experimental procedures

Samples and preparation

A natural sample of manganite (MnOOH) from Wards Natural Science Establishment Inc. was analyzed. Small slabs of the mineral ($0.5 \times 0.5 \times 1$ cm) were cut, fractured within the analytical chamber of the XPS instrument and immediately analyzed to minimize surface contamination. Trivalent Mn is expected (Buerger 1936; Dachs 1962; Dachs 1963; Glausinger et al. 1979). X-ray diffraction powder patterns of our samples indicate only manganite (δ-MnOOH).

Synthetic birnessite films were prepared using a procedure modified after that of Brulé et al. (1980). Small, 1 cm diameter aluminum disks were polished with SiC paper and rinsed with 6 N nitric acid, followed by de-ionized water. After this treatment, the disks were dipped in 1 N $MnSO_4$ solution (pH = 3.85) for 1 min, rinsed with de-ionized water, and dipped in 1 N $KMnO_4$ solution (pH = 3.60) for 1 min. The dipping process was repeated 25 times to produce a dark film of MnO_2 on each disk. When necessary, these samples were stored in de-ionized water and were air-dried before being transferred to the XPS analytical chamber. Maximum storage time was 8 h. A photomicrograph of the film and an enlargement (see Appendix) illustrates the nature of the precipitate. The morphological uniformity of the precipitate (examined by SEM) suggests the presence of only one phase.

Instrumentation

XPS were collected using a modified Surface Science Laboratories SSX-100 X-ray photoelectron spectrometer (Surface Science Center, U.W.O), with a monochromatized Al$K\alpha$ X-ray source and base pressure of 1×10^{-9} Torr in the analytical chamber. The spectrometer work function was adjusted to give 84.00 ± 0.05 eV for the $Au(4f_{7/2})$ peak of metallic gold. The energy dispersion was set to give a difference of 857.5 ± 0.1 eV between the $Cu(2p_{3/2})$ and $Cu(3p)$ lines. Survey scans were recorded using a 600 μm spot size and a fixed pass energy of 160 eV, whereas narrow scans were collected using a 150 μm spot size and a fixed pass energy of 25 eV. X-ray diffraction (XRD) analysis was conducted on powdered samples of manganite. The XRD identification of synthetic birnessite was performed on thickened film precipitated on an aluminum disk. The film was prepared as

previously stated, but over 100 dipping cycles were performed to produce a sufficiently thick birnessite coating on the aluminum disk. A monochromatized Co$K\alpha$ X-ray source was used for the XRD studies, and electron microprobe analyses were collected using a Jeol JXA-8600 Superprobe (Dept. of Earth Sciences, U.W.O).

The average bulk composition (in weight percent) is Mn = 60.6 (s = 0.3, n = 7), Fe = 0.11, Ni = 0.08, Ba = 0.16, K = 0.40, and P = 0.16. The amount of OOH^{3-} required to complete the formula is about 36.6 wt% for a total of 97.9 wt%. The shortfall suggests that H_2O exists in the sample. These natural samples display minimal solid solution. XRD of the same thickened film yielded a pattern identified as 7 Å birnessite. D-values and intensities of the five strongest peaks were 7.3 Å (100), 2.42 Å (90), 2.1 Å (30), 1.27 Å (20), and 4.8 Å (20). Potassium is the only possibility for inclusion in the mineral (from $KMnO_4$), but none was observed in XPS broadscans. The XRD spectrum compares closely with peak positions and intensities obtained by Bricker (1965) for synthetic birnessite (ASTM file No. 18-802). The XRD pattern also is similar to the 7 Å birnessite observed in manganese nodules (Kuma et al. 1994; Burns and Burns 1977; Glasby 1972). As shown subsequently, the composition of birnessite here synthesized is $MnO_{1.95}$, hence is non-stoichiometric and contains Mn^{4+}, Mn^{3+}, and Mn^{2+} in the proportions 70:25:5.

PREVIOUS STUDIES OF Mn(2p) MULTIPLET SPLITTINGS

Introduction

Multiplet splitting of Mn(3s) and Mn(3p) XPS spectral peaks has received considerable attention over the last 25 years (Fadley et al. 1969; Carver et al. 1972; Okada and Kotani 1992; Hermsmeier et al. 1993). Less emphasis has been placed on multiplet peaks contributing to Mn(2p) spectra (Kowalczyk et al. 1975). The complexity of Mn(2p) metal photo-peaks arises from the coupling of angular momenta associated with partially filled core and valence shells containing unpaired electrons. Gupta and Sen (1974, 1975) considered electrostatic, spin-orbit, and crystal field interactions to calculate the 2p multiplet splitting of 36 3-d transition metal free ions. Free ion implies that no electrostatic field is imposed (no associated ligands), hence the free ion is in high spin state. They did not consider configurations other than ground-state and did not investigate satellite structures such as shakeup and shake-off (Carlson 1975, Chap. 5). Although limited, their treatment provides a theoretical basis for interpreting 2p photo-peaks of 3-d ions. Calculated 2p XPS spectra for 12 metal ions are reproduced in Figure 1 (figure after Gupta and Sen 1975). The $2p_{3/2}$ spectra of isoelectronic ions are similar, but vary with the magnitude of the binding energies separating multiplet peaks (energy splittings). Energy splittings increase for ions of successively higher atomic number. Only a few studies have
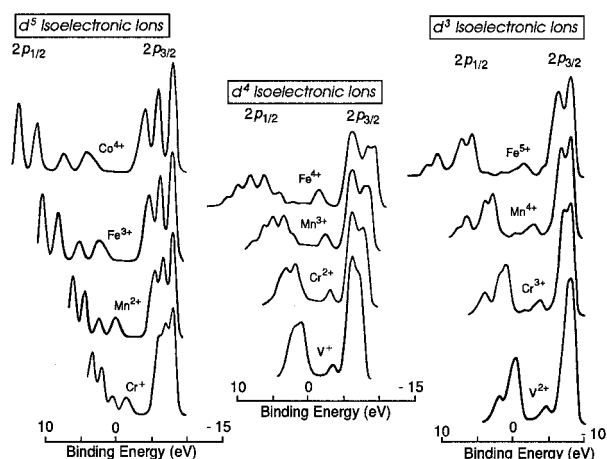
FIGURE 1. XPS 2p multiplet structures for some d⁵, d⁴, and d³ free ions (high spin) calculated by Gupta and Sen (1974, 1975). The calculations are based on electrostatic, spin-orbit, and crystal field interactions.

TABLE 1. Peak parameters for free ions and oxyhydroxides

Peak ID	B.E. (eV)	FWHM (percent)	Intensity*	Comments
Mn(2p) Parameters: Calculated (Gupta and Sen 1974, 1975)				
Mn^{2+}-free Ion	640.0	1.0	100.0	Multiplet no. 1
Mn^{2+}-free Ion	641.3	1.0	75.2	Multiplet no. 2
Mn^{2+}-free Ion	642.4	1.0	50.8	Mulitplet no. 3
Mn^{2+}-free Ion	643.1	1.0	25.2	Multiplet no. 4
Mn^{2+}-free Ion	647.6	1.0	15.0	Multiplet no. 5
Fitted (Fig. 2)				
Mn^{2+}-in MnO	640.0	1.7	100.0	Multiplet no. 1
Mn^{2+}-in MnO	641.2	1.7	76.0	Multiplet no. 2
Mn^{2+}-in MnO	642.0	1.7	49.0	Multiplet no. 3
Mn^{2+}-in MnO	642.9	1.7	25.0	Multiplet no. 4
Mn^{2+}-in MnO	647.5	1.7	10.2	Multiplet no. 5
Mn^{2+}-in MnO	645.0	3.5	30.3	Satellite
Calculated (Gupta and Sen 1974, 1975)				
Mn^{3+}-free Ion	640.7	1.0	100.0	Multiplet no. 1
Mn^{3+}-free Ion	641.4	1.0	100.0	Multiplet no. 2
Mn^{3+}-free Ion	642.3	1.0	135.0	Multiplet no. 3
Mn^{3+}-free Ion	643.1	1.0	70.0	Multiplet no. 4
Mn^{3+}-free Ion	644.9	1.0	30.0	Multiplet no. 5
Fitted (Fig. 3c)				
Mn^{3+}-Manganite	640.7	1.25	100.0	Multiplet no. 1
Mn^{3+}-Manganite	641.4	1.25	100.0	Multiplet no. 2
Mn^{3+}-Manganite	642.2	1.25	116.0	Multiplet no. 3
Mn^{3+}-Manganite	643.2	1.25	73.0	Multiplet no. 4
Mn^{3+}-Manganite	644.6	1.60	28.0	Multiplet no. 5
Calculated (Gupta and Sen 1974, 1975)				
Mn^{4+}-free Ion	641.9	1.0	100.0	Multiplet no. 1
Mn^{4+}-free Ion	642.9	1.0	66.7	Multiplet no. 2
Mn^{4+}-free Ion	643.8	1.0	33.3	Multiplet no. 3
Mn^{4+}-free Ion	644.8	1.0	13.5	Multiplet no. 4
Mn^{4+}-free Ion	646.8	1.0	23.3	Multiplet no. 5
O(1s) Parameters: Fitted (Fig. 5)				
Manganite	529.6	1.20	100.0	O^{2-} structural
Manganite	530.8	1.20	100.0	OH^- structural
Manganite	531.6	1.80	53.1	H_2O structural?
Birnessite	529.6	1.17	100.0	O^{2-} structural
Birnessite	530.9	1.17	13.0	OH^- structural
Birnessite	532.3	1.60	9.8	H_2O sorbed?

* Peak intensities are relative to the intensity of the peak with the lowest binding energy.

attempted to test the validity of the calculations or to use them to interpret 2p XPS spectra of the 3-d metals in solids (Kowalczyk et al. 1975; McIntyre and Zetaruk 1977; Okada and Kotani 1992; Pratt et al. 1994).

Mn(2p) spectrum of Mn²⁺ free ion

The calculated free ion $Mn^{2+}(2p_{3/2})$ spectrum (Gupta and Sen 1974, 1975) yields four major multiplet peaks separated by approximately 1 eV contributing to the $2p_{3/2}$ line. Three of the four peaks are apparent in Figure 1. The fourth peak is of low intensity and expressed in the shallow slope on the high-binding energy side of the $2p_{3/2}$ emission. (An additional peak is located at about 0 eV in Figure 1 and numerous multiplets contribute to the $2p_{1/2}$ line.) Kowalczyk et al. (1975) were the first to confirm the essential validity of the Gupta and Sen calculations for Mn^{2+} $2p_{3/2}$ photo-peaks by studying MnF_2. They successfully fitted the $2p_{3/2}$ peak with multiplets of intensities and energy splittings similar to those calculated by Gupta and Sen (1974). The multiplet peak parameters derived from Gupta and Sen (1974) are listed in Table 1.

Mn^{2+} and Fe^{3+} are isoelectronic. McIntyre and Zetaruk (1977) demonstrated that the $Fe^{3+}(2p_{3/2})$ XPS spectra of Fe^{3+} oxides and oxyhydroxides were composed of multiplet peaks with structures resembling those calculated spectra (Gupta and Sen 1975) and similar to the $Mn(2p_{3/2})$ spectrum of Mn^{2+} in MnF_2 (Kowalczyk et al. 1975). Both Mn^{2+} in MnF_2 and Fe^{3+} in oxyhydroxides are in high spin states. The similarity of calculated and observed 2p Mn^{2+} and Fe^{3+} spectra of oxides and fluorides suggests that calculated spectra of Gupta and Sen (1975) should be a reasonable guide for interpretation of Mn(2p) spectra in Mn^{2+} oxides and oxyhydroxides, provided Mn^{2+} is in the high spin state in the oxide. Okada and Kotani (1992) calculated the $Mn^{2+}(2p_{3/2})$ spectra for MnO (Fig. 2a) and it is similar to the $Mn^{2+}(2p_{3/2})$ spectra in both MnF_2 and MnO (Fig. 2b), as discussed subsequently.

Mn(2p) spectrum of Mn³⁺ free ion

Comparison of the Mn^{3+} and isoelectronic Fe^{4+} free ion spectra (Fig. 1) demonstrates that the lower energy $2p_{3/2}$ peak of the Mn^{3+} free ion has two components. Their intensities are the same and their energy splitting is less than 1 eV leading to a plateau on the low energy side of the $2p_{3/2}$ peak. A third peak is located at somewhat higher binding energy (splitting greater than 1 eV), and it is the most intense of the multiplet peaks. A low intensity fourth peak occurs as a weak shoulder on the high binding energy side of the most intense peak. A fifth broad, low intensity, peak occurs at 2.6 eV greater binding energy than the most intense peak, thus falling between the $2p_{3/2}$ and $2p_{1/2}$ peaks.

Gupta and Sen (1975) constructed the 2p spectral envelope for the Mn^{3+} free ion using a 100% Gaussian peak shape and a FWHM of 1.0 eV. The five peaks previously identified have been assigned these same peak characteristics and peak intensities, and their energies were varied
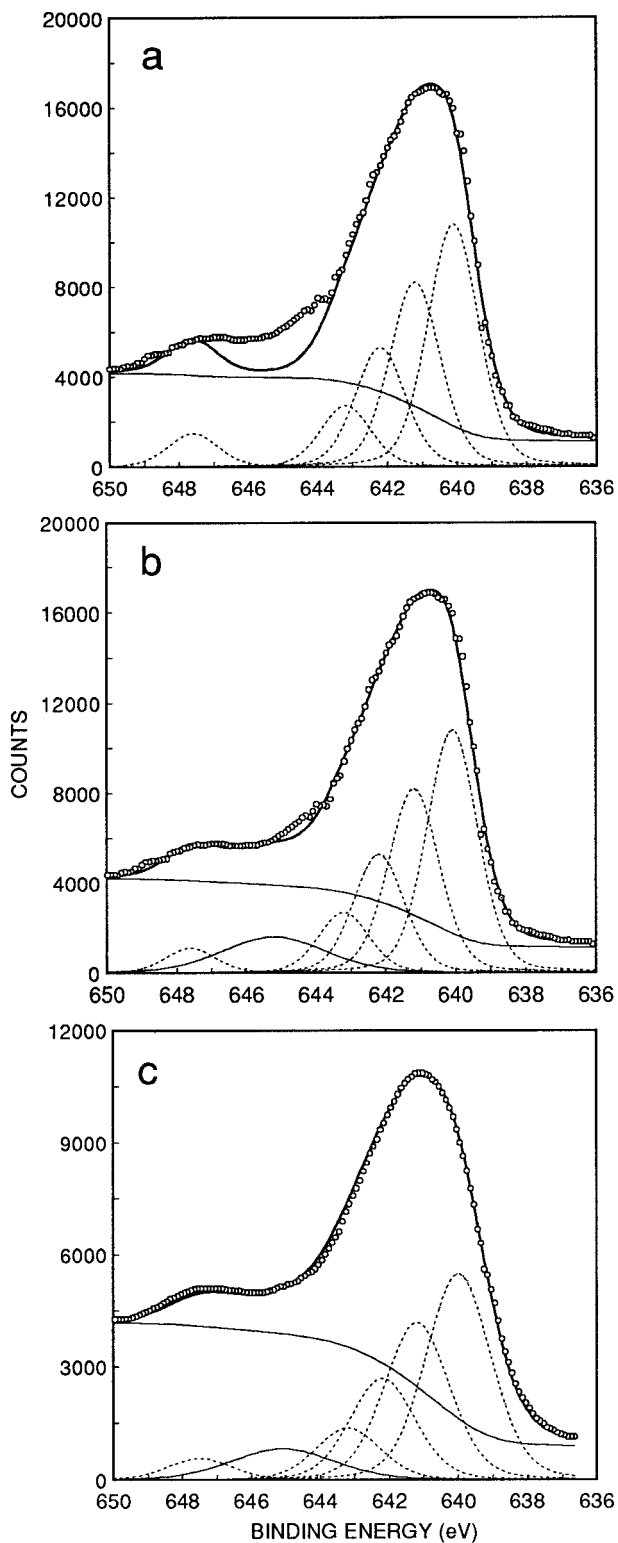
Figure 2. XPS Mn($2p_{3/2}$) spectra of Mn^{2+} in MnO. (**a**) Mn(2p) spectrum collected by Okada and Kotani (1992). The solid curve represents the best fit to the XPS data. The dotted curves represent the fitted Mn($2p_{3/2}$) multiplet peaks. Each fitted peak is predicted by Gupta and Sen (1974, 1975). The poor fit between 644 and 647 eV indicates that there is an additional contribution to the spectrum, as discussed in the text. (**b**) The data, fit, and multiplet peaks are the same as in Figure 2a. There is added, however, an additional peak centered near 645.5 eV illustrated by the thin solid peak. As discussed in the text, it may be a shake-up peak. (**c**) Mn(2p) spectrum collected by Di Castro and Polzonetti (1989) and fitted with the same multiplet peaks and satellite peak as used to fit the spectrum shown in Figure 2b.

←

to yield the $2p_{3/2}$ XPS spectrum of Figure 3a (compare with Mn^{3+} spectrum in Fig. 1). Increasing the FWHM to 1.3 eV and use of a 70% Gaussian-30% Lorentzian peak shape (while maintaining peak energies and intensities) yields the 2p spectrum shown in Figure 3b. Numerous studies document the 2p spectrum of Mn^{3+}-bearing oxides (Table 2), but none has attempted to deconvolute the 2p spectrum into multiplet and satellite structures.
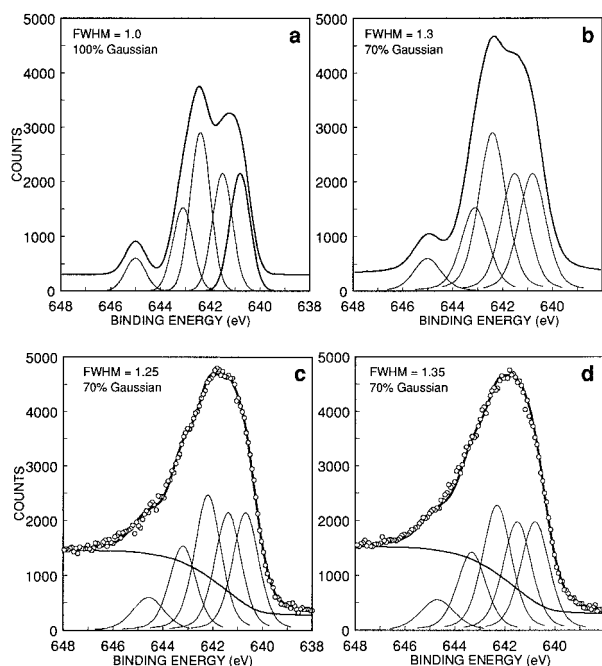
Mn(2p) spectrum of Mn^{4+} free ion

The Mn^{4+}($2p_{3/2}$) spectrum of Gupta and Sen (1975) includes two maxima separated by approximately 1 eV, with the lower binding energy peak being more intense (Figs. 1 and 4a). The slope on the high energy side of the $2p_{3/2}$ peak of Mn^{4+} (and all other d³ isoelectronic ions of Fig. 1) is appreciably shallower than the slope on the low energy side of the peak, indicating the presence of a closely spaced multiplet on the high energy side. A peak has been included in the spectrum of Figure 4a to represent this contribution. As apparent from the isoelectronic Fe(V) free ion $2p_{3/2}$ spectrum (Fig. 1), there are two small peak contributions at approximately 2.6 and 4.6 eV greater energy than the lowest binding energy peak. These are included in Figure 4a.

Gupta and Sen (1975) calculated the 2p spectrum by assigning FWHM of 1.0 eV and 100% Gaussian peak characteristics to each of the five multiplets (Fig. 4a, compare with Fig. 1). A second Mn^{4+} spectrum, with FWHM of 1.3 and 70% Gaussian-30% Lorentzian peak characteristics assigned to the multiplets, is illustrated in Figure 4b.

Mn(2p) XPS spectrum of MnO

Okada and Kotani (1992) calculated the Mn($2p_{3/2}$) spectrum of MnO from theoretical considerations and also collected its spectrum (Fig. 2a). The multiplet peaks and peak parameters provided by Gupta and Sen (1974) were used as a guide to fit the Mn($2p_{3/2}$) XPS peak of MnO (Fig. 2; Table 1) collected by Okada and Kotani (1992). The energy splittings and relative intensities of the multiplet peaks are similar to the calculated values of Gupta and Sen (1974) and are also similar to the energy

FIGURE 3. (a) XPS $Mn(2p_{3/2})$ spectrum of Mn^{3+} free ion calculated by Gupta and Sen (1974, 1975) in which the FWHM of each multiplet peak was assigned a value of 1.0. (b) identical to Figure 3a except the FWHM of each of the multiplet peak is 1.3 eV, which is similar to the FWHM of the Mn^{3+} spectra shown in Figures 3c and 3d. (c) and (d) are two collected XPS $Mn(2p_{3/2})$ spectra of Mn^{3+} in manganite. The peak parameters listed in Table 1 were used to fit the two spectra, with the exception of the FWHM. The FWHM was 1.25 for the fit shown in Figure 3c and 1.35 for the fit shown in Figure 3d.

TABLE 2. $2p_{3/2}$ photo-peak binding energy maxima, oxidation states and coordination of Mn ions in various oxides*

Phase	B.E. (eV)	Oxid. state	Co-ordi-nation	Reference
MnO	641.7	2+	O	Carver et al. 1972
MnO	640.7	2+	O	Oku and Hirokawa 1975
MnO	640.4	2+	O	Oku et al. 1975
MnO	640.9	2+	O	Rao et al. 1979
MnO	640.9	2+	O	Foord et al. 1984
MnO	641.0	2+	O	Di Castro and Polzonetti 1989
$MnCr_2O_4$	640.8	2+	T	Oku and Hirokawa 1975
$MnFe_2O_4$	640.8	2+	T	Brabers et al. 1983
Mn_2TiO_4	640.6	2+	T, O	Brabers et al. 1983
Mn_3O_4	641.4	2+, 3+	T, O	Oku and Hirokawa 1975
Mn_3O_4	641.4	2+, 3+	T, O	Oku et al. 1975
Mn_3O_4	641.7	2+, 3+	T, O	Rao et al. 1979 (shoulder)
Mn_3O_4	641.3	2+, 3+	T, O	Brabers et al. 1983
Mn_3O_4	641.5	2+, 3+	T, O	Di Castro and Polzonetti 1989
Mn_2O_3	641.8	3+	O	Carver et al. 1972
Mn_2O_3	641.9	3+	O	Oku and Hirokawa 1975
Mn_2O_3	641.7	3+	O	Oku and Hirokawa 1975
Mn_2O_3	641.9	3+	O	Oku et al. 1975
Mn_2O_3	641.8	3+	O	Foord et al. 1984
Mn_2O_3	641.9	3+	O	Di Castro and Polzonetti 1989
Mn_2O_3	641.7	3+	O	Rao et al. 1979
$CoMn_2O_4$	641.7	3+	O	Oku and Hirokawa 1975
MnO_2	642.4	4+	O	Carver et al. 1972
MnO_2	642.2	4+	O	Oku et al. 1975
MnO_2	641.9	4+	O	Rao et al. 1979
MnO_2	642.5	4+	O	Foord et al. 1984
MnO_2	642.6	4+	O	Di Castro and Polzonetti 1989
$NiZnMnO_4$	642.5	4+	T	Brabers et al. 1983

* Junta and Hochella (1994) compiled additional data.

splittings and relative peak intensities of Mn^{2+} in MnF_2 (Kowalczyk et al. 1975) as expected in that fluoride (F^-), hydroxide (OH^-), and oxide (O^{2-}) have similar electronegativities (Huheey 1978). Specifically, Mn^{2+} should be in the high spin state in these compounds, hence it should display similar multiplet peak structure.

The $Mn(2p_{3/2})$ XPS spectrum collected by Okada and Kotani (1992) differs in detail from our fitted spectrum, in that only the fit displays a pronounced trough near 645 eV (Fig. 2a). Clearly, contributions to the high energy side of the $Mn(2p_{3/2})$ spectrum cannot be explained by the theoretical considerations of Gupta and Sen (1974, 1975) or Okada and Kotani (1992). Gupta and Sen (1974, 1975) obtained a fifth multiplet peak (Table 1) located at about 8 eV greater binding energy than the most intense peak (Fig. 1). It contributes to the indistinct peak of the XPS data at about 647.5 eV (Fig. 2) but it does not explain the poor fit in the region of 645 eV (Fig. 2a). We consequently surmise that there is a broad peak contributing to the XPS data centered near 645 eV and it may be a shake-up peak. The peak has been included in the fit shown in Figure 2b and is referred to as a satellite peak in Table 1.

To further test the adequacy of the $Mn(2p_{3/2})$ multiplet peak parameters of Table 1, the $Mn(2p_{3/2})$ spectrum of MnO collected by Di Castro and Polzonetti (1989) was fitted with the five multiplet peaks and the satellite peak (Fig. 2c). Peak parameters of Table 1 were used except that the FWHM of each multiplet peak was set to 2.2 because the Di Castro and Polzonetti (1989) spectrum was collected with a nonchromatized Al source. The fit is reasonable and the parameters for the multiplet peaks and the satellite peak listed in Table 1 are adopted to represent $Mn(2p_{3/2})$ spectra for Mn^{2+} in Mn oxides and oxyhydroxides.

Excluding the one extreme value, Mn^{2+} (Table 2), peak energies range from 640.4 to 640.9 eV and the binding energy for the $Mn^{2+}(2p_{3/2})$ peak in MnO is here taken as 640.8 ± 0.3 eV. These values (Table 2) represent the maximum in the $2p_{3/2}$ spectrum rather than the maximum of the most intense multiplet peak. The fitted spectra of Figure 2 indicate that the most intense multiplet peak is located at approximately 0.8 eV lower binding energy than the maximum in the spectrum. This observation, coupled with the average value for the $2p_{3/2}$ peak maximum (640.8 ± 0.3 eV), indicates that the lowest binding energy multiplet peak (and most intense) is located near 640.0 ± 0.3 eV (Table 1). The error associated with peak energy splittings (energy differences between multiplet peaks) is 0.2
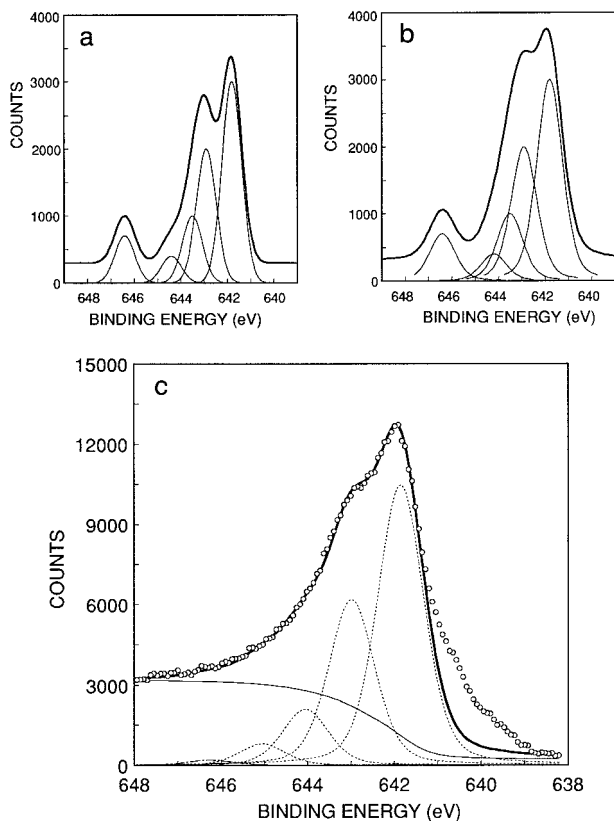
FIGURE 4. (**a**) XPS $Mn(2p_{3/2})$ spectrum of Mn^{4+} free ion calculated by Gupta and Sen (1974, 1975) in which the FWHM of each multiplet peak was assigned a value of 1.0 and the peaks are 100% Gaussian. (**b**) Identical to Figure 3a except the FWHM of each multiplet peak is 1.3 eV and the peak shapes are 70% Gaussian-30% Lorentzian. These peak parameters are similar to those of the Mn^{3+} spectra shown in Figure 3c. (**c**) This is a XPS $Mn(2p_{3/2})$ spectrum of synthetic birnessite. The dots represent the spectral data, the thin solid line the Shirley background, the dotted peaks, the Mn^{4+} multiplet peaks with peak parameters listed in Table 3 used as a guide to fit the high energy side of the spectral data. The thick solid curve represents the $Mn(2p_{3/2})$ spectral fit using only the shown Mn^{4+} multiplet peaks. There is a distinct shoulder between 639 and 641 eV that cannot be attributed to Mn^{4+} muiltiplet peaks (see text).

eV. More precise and accurate evaluation of these binding energies awaits higher resolution studies.

XPS SPECTRA OF MANGANITE

O(1s) Spectrum

The O(1s) spectrum (Fig. 5a) has a maximum near 532 eV, a distinct shoulder on its low binding energy side of the peak, and a pronounced tail on the high energy side. There are, therefore, at least three contributions to the spectrum. Idealized manganite composition requires equal abundance of oxide (O^{2-}) and hydroxide (OH^-), hence equal contributions of these species to the O(1s) spectrum (Fig. 5a).

The spectrum was fitted by constraining O^{2-} and OH^-
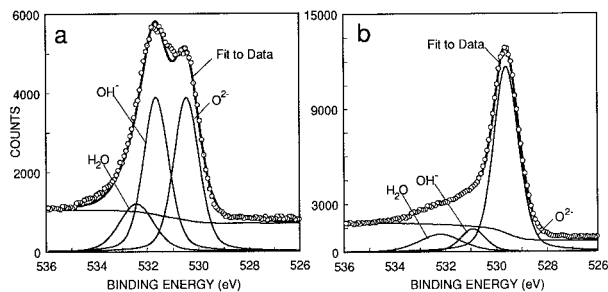
FIGURE 5. (**a**) XPS O(1s) spectrum of manganite. Dots represent the spectral data. The three spectral peaks contributing to the spectrum are labeled, and the near-horizontal line represents the Shirley background. The thick solid curve is the best fit to the spectral data that could be obtained with the oxide and hydroxide peaks constrained to equal intensities. (**b**) The XPS O(1s) spectrum of synthetic birnessite. Symbols and curves are as in (**a**).

peaks to equal intensities and FWHM values. The binding energy separating the two peaks was varied. The FWHM was also varied between 1.1 and 1.2 eV to optimize the fit. The high energy tail may include physisorbed, chemisorbed, and structural H_2O and water in poor electrical contact with the mineral surface (McIntyre and Zetaruk 1977; Pratt et al. 1994; Knipe et al. 1994). These various H_2O contributions cannot be fitted in an unambiguous way; consequently they are represented by one broad peak with FWHM of 1.8 eV. Its intensity and binding energy were adjusted to fit the high energy tail. Fit parameters are listed in Table 1.

The fit to the O(1s) spectrum is reasonable (Fig. 5a) and demonstrates that O^{2-} and OH^- are present in near-equal amounts. The binding energy of the H_2O peak is low (532.3 eV) suggesting that the water is largely chemisorbed or structurally bound (McIntyre and Zetaruk 1977; Pratt et al. 1994). Alternatively, the 532.3 eV peak may represent a second hydroxide peak that is energetically (and presumably structurally) distinct from the manganite-like hydroxide in the near-surface.

Mn($2p_{3/2}$) spectrum

The calculated $Mn^{3+}(2p_{3/2})$ free ion spectrum and the $Mn(2p_{3/2})$ XPS spectra of manganite are reproduced in Figures 3a to 3d. The spectral properties of the multiplet peaks for the Mn^{3+} free ion (Gupta and Sen 1975) in Table 1 were used to initiate fitting of the manganite spectra (Figs. 3c and 3d). The following constraints were used. The two multiplet peaks of lowest binding energy were assigned the same intensities (Fig. 3c). The third peak was constrained to a higher intensity than the two lower binding energy peaks, and the two peaks at highest binding energy were constrained to lower intensities than the three other peaks. The FWHM of these four multiplet peaks was set to 1.25 eV. This value was adopted because the intrinsic line width of the Mn(2p) peak is 0.05 to 0.1 eV greater than the intrinsic width of the O^{2-} peak of the O(1s) spectrum (1.17 eV, Table 1). The fifth multiplet (highest binding energy peak) is broad in the calculated
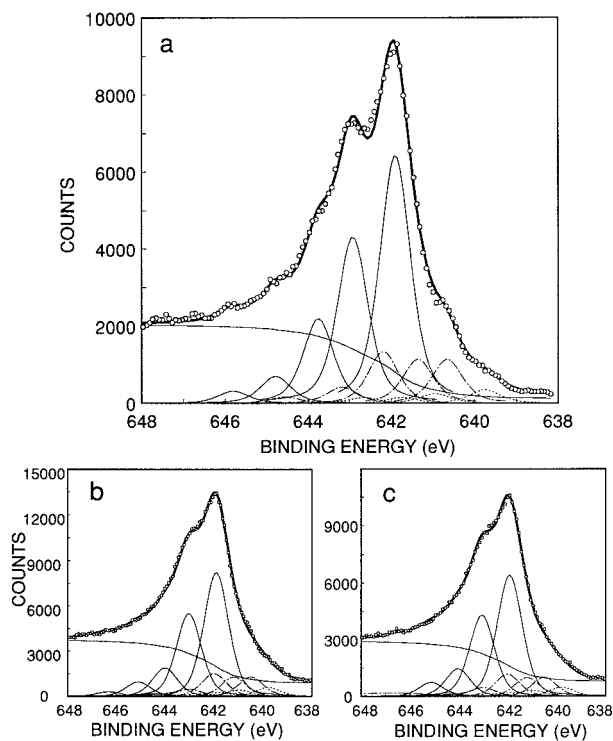
FIGURE 6. (**a**) $Mn(2p_{3/2})$ XPS spectrum of birnessite shown in Figure 4c, enhanced using the maximum entropy method (S.J. Splinter and N.S. McIntyre, unpublished manuscript 1998; Vasquez et al. 1981) to remove much of the Gaussian component of the spectrum. The FWHM of the fitted peaks has decreased from 1.25 eV (Fig. 4c) to 0.87 eV (Fig. 7a) and as a result the enhanced spectrum displays two distinct peaks and a strong low energy shoulder that although evident in Figure 4c, were not strongly developed. The peaks shown by the thin solid lines are Mn^{4+} mulptiplets the parameters of which are listed in Table 3. The dot-dash peaks are Mn^{3+} multiplet peaks and the dotted peaks represent Mn^{2+} photo-peaks. The Shirley background is shown as a thin sigmoidal solid curve and the fit to the spectral data is shown by the thick solid curve (**b**) and (**c**). Two $Mn(2p_{3/2})$ XPS spectra of synthetic birnessite which illustrate reproducibility of $Mn(2p)$ results. Symbols and curves are as in (**a**).

spectrum, and its FWHM was consequently constrained to 1.60 eV. Reasonable fits to the two spectra result (Figs. 3c and 3d), using the peak parameters listed in Table 1.

The fitted multiplet structure is similar to that of the free ion (compare Fig. 3b with Figs. 3c and 3d) but minor differences exist. Whereas the strongest multiplet of Figure 3b is 1.35 times more intense than the lowest binding energy peak, the strongest peaks of Figures 3c and 3d are only 1.16 times more intense. The result is that the peak is flat-topped in Figures 3c or 3d, rather than displaying a distinct peak with a shoulder on its low binding energy side (Fig. 3b). The fitted binding energies differ from those used to construct Figures 3a and 3b by no more than 0.25 eV, and relative intensities differ by no more than 15%. The agreement suggests that the essential features of the Mn^{3+} free ion multiplet structure calculated

by Gupta and Sen (1975) are similar to the $Mn^{3+}(2p_{3/2})$ multiplet structure of manganite.

The $Mn^{3+}(2p_{3/2})$ peak maxima for manganite are 641.7 ± 0.1 (Fig. 3c) and 641.8 ± 0.1 eV (Fig. 3d). The range of eight previous studies of Mn^{3+} oxides is 641.7 to 641.9 eV with an average of 641.8 eV (Table 2). The $Mn^{3+}(2p_{3/2})$ peak maxima in Mn_2O_3 and manganite are 1.0 eV greater than the peak maximum for the $Mn^{2+}(2p_{3/2})$ spectrum of MnO.

XPS SPECTRA OF SYNTHETIC BIRNESSITE

O(1s) spectrum

The O(1s) spectrum (Fig. 5b) of synthetic birnessite has a maximum near 529.6 eV and a distinct, broad shoulder on the high binding energy side of the peak, making it markedly different from the manganite spectrum (Fig. 5a). Peak parameters used to fit the O(1s) spectrum of manganite were employed as initial estimates to fit the spectrum of the birnessite spectrum. The fitted peak parameters are listed in Table 1. Oxide (O^{2-}) constitutes 81.4% of the O(1s) spectrum, OH^- 10.6%, and the remainder is H_2O (chemisorbed, physisorbed, or bound H_2O, McIntyre and Zetaruk 1977; Pratt et al. 1994). The similarity of OH^--binding energies in MnOOH and in the birnessite film suggests that OH^- is structurally bound in birnessite, just as it is in manganite. If so, charge compensation is required to maintain electrical neutrality.

Mn(2p_{3/2}) spectrum

Evidence for Mn^{4+}. The $Mn(2p_{3/2})$ spectrum of synthetic birnessite (Fig. 4c) displays a narrow peak maximum near 642 eV, a distinct shoulder near 643 eV, and a broad, pronounced shoulder between 644 and 647 eV. These features are also present in the calculated Mn^{4+} spectrum (Gupta and Sen 1974, 1975), as shown in Figures 4a and 4b. The similarity of Figures 4b and 4c and the high binding energy of the peak maximum (642 eV), compared with binding energy maxima for MnO and manganite, indicate that Mn^{4+} makes a strong contribution to the synthetic birnessite spectrum (Fig. 4c). The calculated Mn^{4+} free ion spectrum of Figure 4b was used as a guide to fit the $Mn(2p_{3/2})$ spectrum of synthetic birnessite. As shown in Figure 4c, Mn^{4+} multiplet peaks of character similar to those of Figure 4b provide a reasonable fit to the high energy portion of the spectrum. There is, however, a low binding energy shoulder (639 to 641 eV) that cannot be attributed to Mn^{4+} multiplet peaks. The shoulder at low binding energy may include contributions from Mn^{3+} or Mn^{2+} multiplet peaks that are located at lower binding energies than the Mn^{4+} multiplets.

Contributions to the spectrum. Resolution of the $Mn(2p_{3/2})$ XPS spectrum of birnessite was enhanced using the maximum entropy method (Pratt et al. 1998; S.J. Splinter and N.S. McIntyre, unpublished manuscript 1998; Vasquez et al. 1981) to remove much of the Gaussian component of the spectrum. The result is shown in Figure 6a (compare with Fig. 4c). The enhanced spectrum yields a small, but distinct peak near 643 eV on the high

energy shoulder of the main peak. There also is a distinct shoulder developed on the low energy side of the peak that, as presently discussed, may represent Mn in lower oxidation states.

Synthetic birnessite precipitation involves oxidation of Mn^{2+} to Mn^{4+}. The reaction is likely to proceed by the oxidative intermediate Mn^{3+} (fundamental reactions generally proceed as one-electron transfers), hence incompletely oxidized Mn^{3+} may be incorporated into the near-surface of the precipitate. To test this possibility, the low binding energy shoulder was fitted using the Mn^{3+} multiplet peak parameters derived from manganite and listed in Table 1.

Inclusion of both Mn^{4+} and Mn^{3+} multiplet peaks provides a reasonable fit to the $Mn(2p_{3/2})$ spectrum but there remains a small component of the low energy tail, near 639.7 eV, which could not be ascribed to either of these contributions. The energy is indicative of a Mn^{2+} contribution to the spectrum. Addition of the Mn^{2+} multiplet structure yields an excellent fit (Fig. 6) as now discussed.

Estimation of Mn^{4+} peak parameters. The parameters of the $Mn^{4+}(2p_{3/2})$ multiplet peaks have been estimated from the sharpened spectrum shown in Figure 6. The FWHM of all peaks were constrained to 0.87 eV (Fig. 6) and a 50% Gaussian-50% Lorentzian peak shape was assigned to all peaks. The relative intensities and energy splittings for the Mn^{2+} and Mn^{3+} multiplets listed in Table 1 were adopted without modification. Only the intensity and binding energy of the lowest energy peak of each multiplet set were adjusted, thus reducing to two, the number of adjustable parameters available to fit the entire Mn^{2+} and Mn^{3+} multiplet structures to the low energy side of the $Mn(2p)$ peak. The energies and relative intensities derived from the calculated Mn^{4+} free ion (Figs. 4a and 4b) were employed as initial estimates to fit the remainder of the $Mn(2p_{3/2})$ spectrum. The resulting fit is shown in Figure 6 by the solid curve intersecting the spectral data. The fit parameters for Mn^{2+}, Mn^{3+}, and Mn^{4+} are listed in Table 3. The best fit is obtained with the binding energies of the Mn^{2+} and Mn^{3+} multiplet peaks shifted 0.25 eV (to 639.75 eV) and 0.05 eV (to 640.65 eV), respectively, relative to the binding energy of Mn^{2+} in MnO and Mn^{3+} in manganite (Table 1). The fit indicates about 5, 25, and 70 at%, respectively, of Mn^{2+}, Mn^{3+}, and Mn^{4+} in synthetic birnessite (Table 3). The same parameters have been used to fit the unsharpened spectra of two separate preparations of synthetic birnessite and the results are shown in Figures 6b and 6c. The successful fits demonstrate that the peak parameters are reasonable and also demonstrate that separate preparations of synthetic birnessite yield sensibly identical results. The peak parameters for Mn^{4+} multiplets are subject to revision by study of natural or synthetic samples containing a higher proportion of tetravalent manganese.

Six studies report the peak maximum for the $Mn(2p)$ spectrum of MnO_2 (Table 2). Agreement among the studies is reasonable with an average binding energy of 642.3 ± 0.3 eV. The average also agrees with the peak maximum observed for birnessite (642.0 ± 0.1 eV) of Figure

6. None of the referenced studies attempted to deconvolute the $Mn^{4+}(2p_{3/2})$ spectrum into its multiplet and satellite peaks.

DISCUSSION AND CONCLUSIONS

Comparison with other results

Manceau et al. (1992), using XANES, suggested that Mn^{2+} and Mn^{3+} constitute a low percentage of total Mn in vernadite, δ-MnO_2, asbolane and birnessite. Our high resolution XPS results demonstrate that appreciable amounts of Mn^{3+} and Mn^{2+} are present in the near-surface of synthetic birnessite. The inability of Manceau et al. (1992) to resolve the three Mn states may be a result of small binding energy splittings between Mn^{4+}, Mn^{3+}, Mn^{2+}, and MnK edge lines, compounded by broad lines resulting from multiplet splitting. Multiplet splitting has greater broadening effect on MnK edge XANES than Mn2p XPS spectra in that coupling of core and antibonding orbital electrons occur in the former giving rise to multiplets absent in the Mn2p lines. In fact, Manceau et al. (1992) quote experimental line widths should be 1.2 to 1.3 eV yet their actual linewidths (FWHM) are near 2 eV. The unexplained broadening may result from multiplet splitting.

The higher resolution XPS results (FWHM = 0.87 eV) are more reliable regarding chemical state information but our results are restricted to the uppermost 25 Å of the mineral. XANES samples probe more deeply. If, as suggested by Manceau et al. (1992), there is little Mn^{3+} or Mn^{2+} in bulk birnessite, then the near-surface of synthetic birnessite is enriched in Mn^{3+} relative to the bulk phase.

Substitutions in synthetic birnessite

The presence of appreciable Mn^{3+} in the $Mn(2p)$ spectrum (Fig. 6) is evidence that oxidation proceeds by one-electron steps. High resolution SEM images (Fig. 6b) indicate one phase rather than a mixture of phases and XRD indicates synthetic birnessite. Combined, these data demonstrate that Mn^{3+} is incorporated into synthetic birnessite.

About 95% of the $Mn(2p)$ photoelectron signal is derived from a depth less than about 25 Å for these analytical conditions (Tanuma et al. 1991; Mycroft et al. 1995). The XPS signal derived from the surface layer should contribute about 20% of the total $Mn(2p)$ signal. The Mn^{2+} contribution to the total $Mn(2p)$ signal is only 5% (Table 4) so that the entire Mn^{2+} signal may be derived from the surface layer. Mn^{2+} is 45% larger than Mn^{4+} (Shannon 1976) so that substitution of Mn^{2+} on Mn^{4+} sites in synthetic birnessite is unlikely. Mn^{2+} may therefore be restricted to surface and interlayer positions.

The Mn^{3+} contribution represents about 25% of the total Mn signal (Table 3). It is unlikely to be confined to the surface layer. The radius of Mn^{3+} is 0.785 Å whereas Mn^{4+} is 0.67 Å (both in sixfold coordination and high spin states, Shannon 1976). Consequently, substitution of Mn^{3+} for Mn^{4+} in synthetic birnessite is feasible provided that charge compensation is achieved. A substitution scheme consistent with these considerations, while maintaining the Mn^{4+},

TABLE 3. Mn($2p_{3/2}$) peak parameters for Mn in birnessite films

Peak	B.E.* (eV)	FWHM† (eV)	Percent‡ (%)	Surface species and comments
Mn²⁺($2p_{3/2}$) Parameters: Mn²⁺(total) = 4.9 ± 0.1 At. Pct.				
Mn²⁺	639.75	0.87	1.80	Mn²⁺-O Multiplet no. 1
Mn²⁺	640.95	0.87	1.28	Mn²⁺-O Multiplet no. 2
Mn²⁺	641.75	0.87	0.75	Mn²⁺-O Multiplet no. 3
Mn²⁺	642.65	0.87	0.54	Mn²⁺-O Multiplet no. 4
Mn²⁺	644.15	0.87	0.54	Mn²⁺-O Multiplet no. 5
Mn³⁺($2p_{3/2}$) Parameters: Mn³⁺(total) = 24.7 ± 0.3 At. Pct.				
Mn³⁺	640.65	0.87	5.92	Mn³⁺-O Multiplet no. 1
Mn³⁺	641.35	0.87	5.92	Mn³⁺-O Multiplet no. 2
Mn³⁺	642.16	0.87	6.87	Mn³⁺-O Multiplet no. 3
Mn³⁺	643.18	0.87	4.32	Mn³⁺-O Multiplet no. 4
Mn³⁺	644.55	0.87	1.66	Mn³⁺-O Multiplet no. 5
Mn⁴⁺($2p_{3/2}$) Parameters: Mn⁴⁺(total) = 70.4 ± 0.3 At. Pct.				
Mn⁴⁺	641.90	0.87	33.22	Mn⁴⁺-O Multiplet no. 1
Mn⁴⁺	642.92	0.87	21.26	Mn⁴⁺-O Multiplet no. 2
Mn⁴⁺	643.75	0.87	10.62	Mn⁴⁺-O Multiplet no. 3
Mn⁴⁺	644.78	0.87	3.32	Mn⁴⁺-O Multiplet no. 4
Mn⁴⁺	645.80	0.87	1.99	Mn⁴⁺-O Multiplet no. 5

* Binding energies are significant to 0.1 eV but an additional figure is added because energy splittings are much more accurate than the absolute binding energies.
† All peaks modeled as 50% Gaussian–50% Lorentzian.
‡ The percentage represents the contribution of each peak to the total number of counts under the Mn($2p_{3/2}$) peak.

Mn³⁺, and Mn²⁺ proportions observed in the Mn(2p) XPS spectrum (Fig. 6), requires Mn³⁺ to occupy cationic sites with hydroxide substituted for oxide on anionic sites to maintain charge balance (e.g., the MnOOH component is included in synthetic birnessite as an essential constituent). Mn²⁺ is also included (here as an MnO component) although it may be restricted to the near-surface. The resulting composition is $(Mn_{0.7}^{4+}Mn_{0.25}^{3+}Mn_{0.05}^{2+})_1O_{1.7}(OH)_{0.25}$ or $MnO_{1.95}$ if hydrogen is ignored. The synthetic phase is nonstoichiometric. Hydroxide represents 12.5% of total O for this composition. The O in hydroxide, measured from the O(1s) spectrum (Fig. 5b), is approximately 12.3% (the fit allows a minimum of 10% and a maximum of 15% OH⁻). The O(1s) data provide independent confirmation of the veracity of the proposed components.

Formation of Mn³⁺-bearing birnessite

Reaction of permanganate (MnO_4^-) with Mn²⁺ in aqueous acidic solutions produces $MnO_2(s)$, as observed here and by others (Polissar 1935), with the following formal stoichiometry:

$$2MnO_4^- + 3Mn^{2+} + 2H_2O \rightarrow 5MnO_2(s) + 4H^+. \quad (1)$$
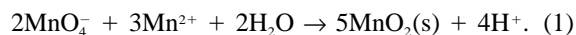
All Mn of the dioxide is considered (for convenience) to be Mn⁴⁺. It is a classical, non-complementary electron transfer reaction that proceeds by a series of elementary steps with each step generally involving transfer of only one electron (Espenson 1970; Purcell and Kotz 1977). When one-electron transfer occurs, a variety of species with intermediate oxidation states are produced, including Mn⁶⁺ (MnO_4^{2-}), Mn⁵⁺ (MnO_4^{3-}), Mn⁴⁺ (precipitated as birnessite), and Mn³⁺ [Mn³⁺(aq) or MnOOH precipitate]. All have been observed in nature or in the laboratory (Cotton

and Wilkinson 1988). Pathways for their production are now discussed.

Mn³⁺ may form through a one electron transfer between permanganate and Mn²⁺, as postulated by Polissar (1935) from his kinetic study:

$$MnO_4^- + Mn^{2+}(aq) \rightarrow MnO_4^{2-} + Mn^{3+}(aq). \quad (2)$$

As support, manganate (MnO_4^{2-}) forms through reduction of permanganate (Sheppard and Wahl 1957). Mn³⁺(aq) of Equation 2 disproportionates (Diebler and Sutin 1964), the stoichiometry of which is:

$$2Mn^{3+}(aq) + 2H_2O \rightarrow MnO_2(s) + Mn^{2+}(aq) + 4H^+. \quad (3)$$

The reaction produces birnessite and replenishes Mn²⁺. According to Cotton and Wilkinson (1988, p. 708), manganate ion also disproportionates rapidly in acidic solutions (as used here):

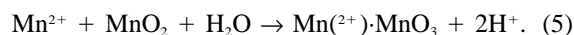$$3MnO_4^{2-} + 4H^+ \rightarrow 2MnO_4^- + MnO_2(s) + 2H_2O. \quad (4)$$
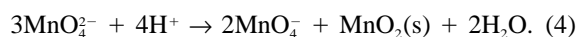
Birnessite formation therefore may occur by two pathways represented by Equations 3 and 4. During reaction, however, Mn³⁺ and birnessite are produced simultaneously. Mn³⁺ probably is produced at the surface of the precipitate, where it is available to be taken into the solid. The low solubility of Mn³⁺-oxyhydroxides (Bricker 1965) probably prevents it from being released to solution, thus promoting its incorporation into the solid.
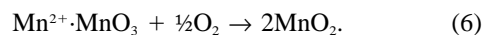
Polissar (1935) was the first to observe that precipitation of MnO_2 (Eq. 1) was autocatalytic in that the reaction was enhanced by increased abundance of the precipitate. This same effect has been observed for other systems where Mn³⁺ is present. Junta and Hochella (1994) note that Mn³⁺-oxyhydroxide has a strong autocatalytic effect on Mn²⁺(aq) oxidation at goethite surfaces. Mn³⁺ in synthetic birnessite may have a similarly pronounced catalytic effect.

Rate equation and surface reactions

Previous studies. Polissar (1935), Morgan and Stumm, (1964), Morgan (1967), Coughlin and Matsui (1976), Hem (1981), Hem and Lind (1983), and Davies and Morgan (1989) studied the kinetics of Mn oxidation and precipitation. The results are summarized in the rate equation proposed by Davies and Morgan (1989). The rate expression indicates an induction period during which a MnO_2 substrate is formed. As the amount of precipitated birnessite is increased, its rate of its precipitation accelerates (autocatalytic), as expressed by the second term of the rate equation. Stumm and Morgan (1981) first introduced the autocatalytic term, but they qualified their interpretation by stating that "the reaction might be visualized to proceed according to the following pattern:"

$$Mn^{2+} + MnO_2 + H_2O \rightarrow Mn^{(2+)} \cdot MnO_3 + 2H^+. \quad (5)$$

followed by:

$$Mn^{2+} \cdot MnO_3 + \tfrac{1}{2}O_2 \rightarrow 2MnO_2. \quad (6)$$

Stumm and Morgan (1981) clearly did not suggest that Reactions 5 and 6 were elementary reactions. Further-
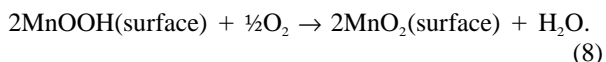
more, they emphasized that the reactions are unbalanced (but are balanced here). In an attempt to further constrain the nature of the elementary steps, the implications of our XPS results are incorporated into the argument of Stumm and Morgan (1981) and Davies and Morgan (1989).

Constraints on charge transfer reactions. Reaction 6 implies simultaneous transfer of two electrons during one reaction step. It is therefore unlikely to be an elementary charge transfer reaction because the probability of more than one electron being transferred during one elementary step is remote. If transfer of only one electron per elementary reaction is adopted, then oxidation of $Mn^{2+}(aq)$ by any oxidant (e.g., O_2), to produce MnO_2 requires formation of an intermediate reaction product containing Mn^{3+}. This, in turn, implies that the Reaction 6 includes at least two elementary steps, one to produce Mn^{3+} from $Mn^{2+}(aq)$ and a second to produce Mn^{4+} (as MnO_2) from the Mn^{3+}-bearing intermediate product. The nature of the Mn^{3+}-bearing intermediate is not certain, but Mn^{3+}-oxyhydroxide is an essential constituent in synthetic birnessite of our experiments and is a likely candidate. Once the Mn^{3+}-bearing intermediate is formed, most Mn^{3+} is subsequently oxidized to MnO_2 but some may remain as Mn^{3+} to be incorporated into birnessite. A scheme is proposed that incorporates these and previous considerations.

The ambiguities associated with reaction 6 are overcome if, after adsorption of Mn^{2+} onto the birnessite surface (to produce $Mn^{2+} \cdot MnO_3$), an Mn^{3+}-oxyhydroxide surface species is produced according to:

$$Mn^{2+} \cdot MnO_3(surface) + H_2O \rightarrow 2MnOOH(surface) \quad (7)$$
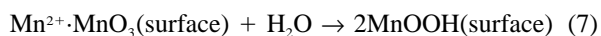
followed by oxidation of the surface MnOOH species:

$$2MnOOH(surface) + \tfrac{1}{2}O_2 \rightarrow 2MnO_2(surface) + H_2O. \quad (8)$$

The sum of these two equations yields Reaction 6. The XPS studies here suggest that the intermediate is an Mn^{3+}-oxyhydroxide, perhaps MnOOH. One of surface Reactions 7 or 8 probably controls the rate of formation of synthetic birnessite during the autocatalytic stage.

These modifications are consistent with the rate equation for the autocatalytic step proposed by Stumm and Morgan (1981) and as expressed by Davies and Morgan (1989). They are also consistent with the XPS results reported here, with the results of Junta and Hochella (1994), and with the results of Coughlin and Matsui (1976). Although Reactions 7 and 8 are more likely to be elementary reactions than is Reaction 6, new studies may show them to be stoichiometric. They nevertheless represent an advance toward elucidation of the elementary reactions.

Surface sites and surface area. These surface analytical studies and the study of Junta and Hochella (1994) demonstrate that surface area alone is insufficient to evaluate the nature and rates of surface reactions. Just as important is the measurement and quantification of the number of surface reactive sites per unit surface area and the oxidation state of transition metal ions at metal oxide surfaces. In this regard, the oxidation states of Mn, partic-

ularly the surface density of Mn^{3+} species, are required in that the latter is a measure of the concentration of the reactive, surface intermediate reaction product. BET and similar measurements do not reflect Mn^{3+}-oxyhydroxide surface concentration on birnessite surfaces and may not be reliable measures of reactive species at solid surfaces. XPS measurements can be used to determine the oxidation states of constituents at mineral surfaces and to quantify their proportions. Electrochemical and corrosion studies now routinely include surface analysis to interpret their results. Geochemists conducting dissolution and kinetic investigations must follow their lead.

REFERENCES CITED

Brabers, V.A.M., van Setten, F.M., and Knapen, P.S.A. (1983) X-ray photoelectron spectroscopy study of the cation valencies in nickel manganite. Journal of Solid State Chemistry, 49, 93–98.

Bricker, O.P. (1965) Some stability relations in the system Mn-O₂-H₂O at 25° and one atmosphere total pressure. American Mineralogist, 50, 1296–1354.

Brulé, D.G., Brown, J.R., Bancroft, G.M., and Fyfe, W.S. (1980) Cation adsorption by hydrous manganese dioxide: a semi-quantitative X-ray photoelectron spectroscopic (ESCA) study. Chemical Geology, 28, 331–339.

Buerger, M.J. (1936) The symmetry and crystal structure of manganite, Mn(OH)O. Zeitschrift für Kristallographie, 95, 163–174.

Burns, R.G. and Burns, V.M. (1977) The mineralogy and crystal chemistry of deep-sea manganese nodules, a polymetallic resource of the twenty-first century. Philisophical Transactions of the Royal Society of London, A, 286, 283–301.

Carlson, T.A. (1975) Photoelectron and Auger Spectroscopy, 417 p. Plenum Press, New York.

Carver, J.C., Schweitzer, G.K., and Carlson, T.A. (1972) Use of X-ray photoelectron spectroscopy to study bonding in Cr, Mn, Fe, and Co compounds. Journal of Chemical Physics, 57, 973–982.

Cotton, F.A. and Wilkinson, G. (1988) Advanced Inorganic Chemistry (fifth edition), 1455 p. Wiley, New York.

Coughlin, R.W. and Matsui, I. (1976) Catalytic oxidation of aqueous Mn(II). Journal of Catalysis, 41, 108–123.

Dachs, H. (1962) Determination of the hydrogen positions in manganite, MnOOH, with neutron diffraction. Journal of the Physical Society of Japan, suppl. 17, B-II, 387–389.

Dachs, H. (1963) Neutronen und Rontgenuntersuchungen am Manganit, MnOOH. Zeitschrift für Kristallographie, 118, 303–326.

Davies, S.H.R. and Morgan, J.J. (1989) Manganese (II) oxidation kinetics on metal oxide surfaces. Journal of Colloidal and Interface Science, 129, 63–77.

Di Castro, V. and Polzonetti, G. (1989) XPS study of MnO Oxidation. Journal of Electron Spectroscopy and Related Phenomena, 48, 117–123.

Diebler, H. and Sutin, N. (1964) The kinetics of some oxidation-reduction reactions involving Manganese (III). Journal Physical Chemistry, 68, 174–180.

Espenson, J.H. (1970) Oxidation of transition metal complexes by chromium (VI). Accounts of Chemical Research, 3, 347–353.

Fadley, C.S., Shirley, D.A., Freeman, A.J., Bagus, P.S., and Mallow, J.V. (1969) Multiplet splitting of core-electron binding enrgies in transition-metal ions. Physical Review Letters, 23, 1397–1401.

Foord, J.S., Jackman, R.B., and Allen, G.C. (1984) An X-ray photoelectron spectroscopic investigation of the oxidation of manganese. Philosophical Magazine, A 49, 657–663.

Glasby, G.P. (1972) The mineralogy of manganese nodules from a range of marine environments. Marine Geology, 13, 57–72.

Glausinger, W.S., Horowitz, H.S., and Longo, J.M. (1979) Preparation and magnetic properties of manganite. Journal of Solid State Chemistry, 29, 117–120.

Gupta, R.P. and Sen, S.K. (1974) Calculations of multiplet structure of core p-vacancy levels. Physical Reviews B, 10, 71–79.

———(1975) Calculations of multiplet structure of p-vacancy levels. II. Physical Reviews B, 12, 15–19.

Hem, J.D. (1981) Rates of manganese oxidation in aqueous systems. Geochimica Cosmochimica Acta, 45, 1369–1374.

Hem, J.D. and Lind, C.J. (1983) Nonequilibrium models for predicting forms of precipitated manganese oxides. Geochimica Cosmochimica Acta, 47, 2037–2046.

Hermsmeier, B.D., Fadley, C.S., Sinkovic, B., Krause, M.O., Jimenez-Mier, J., Gerard, P., Carlson, T.A., Manson, S.T., and Bhattacharya, S.K. (1993) Energy dependence of the outer core-level multiplet structures in atomic Mn and Mn-containing compounds. Physical Reviews B, 48, 12425–12437.

Huheey, J.E. (1978) Inorganic Chemistry (2nd edition), 889 p. Harper and Row, New York.

Junta, J.L. and Hochella, M.F. (1994) Manganese (II) oxidation at mineral surfaces: a microscopic and spectroscopic study. Geochimica Cosmochimica Acta, 58, 4985–4999.

Junta, J.L., Hochella, M.F., Harris, D.W., and Edgell, M. (1992) Manganese oxidation at mineral-water interfaces, a spectroscopic approach. In Y.K. Kharaka and A.S. Maest, Eds., Water-Rock Interaction WRI-7, p. 163–166, A.A. Balkema, Amsterdam.

Knipe, S.W., Mycroft, J.R., Pratt, A.R., Nesbitt, H.W., and Bancroft, G.M. (1994) X-ray photoelectron spectroscopic study of water adsorption on iron sulphide minerals. Geochimica Cosmochimica Acta, 59, 1079–1090.

Kowalczyk, S.P., Ley, L., McFeely, F.R., and Shirley, D.A. (1975) Multiplet splitting of the manganese 2p and 2p levels in MnF₂ single crystals. Physical Reviews B, 11, 1721–1727.

Kuma, K., Usui, A., Paplawsky, W., Gedulin, B., and Arrhenius, G. (1994) Crystal structures of synthetic 7 Å and 10 Å manganates substituted by mono- and divalent cations. Mineralogical Magazine, 58, 425–447.

Manceau, A., Gorshkov, A.I., and Drits, V.A. (1992) Structural chemistry of Mn, Fe, Co, and Ni in manganese hydrous oxides: Part I. Information from XANES spectroscopy. American Mineralogist, 77, 1133–1143.

McIntyre, N.S. and Zetaruk, D.G. (1977) X-ray photoelectron spectroscopy studies of iron oxides. Analytical Chemistry, 49, 1521–1529.

Morgan, J.J. (1967) Chemical equilibria and kinetic proporties of manganese in natural waters. In S.D. Faust and J.V. Hunter, Eds., Principles and Application of Water Chemistry, p. 561–626, Wiley, New York.

Morgan, J.J. and Stumm, W. (1964) Colloid-chemical properties of manganese dioxide. Journal Colloid Science 19, 347–359.

Murray, J.W., Dillard, J.G., Giovanoli, R., Moers, H., and Stumm, W. (1985) Oxidation of Mn(II): Initial mineralogy, oxidation state and ageing. Geochimica Cosmochimica Acta, 49, 463–470.

Mycroft, J.R., Nesbitt, H.W., and Pratt, A.R. (1995) X-ray photoelectron and Auger electron spectroscopy of air-oxidized pyrrhotite: Distribution of oxidized species with depth. Geochimica Cosmochimica Acta, 59, 721–733.

Okada, K. and Kotani, A. (1992) Interatomic and intra-atomic configuration interactions in core-level X-Ray photoemission spectra of late transtion-metal compounds. Journal of the Physical Society of Japan, 61, 4619–4637.

Oku, M. and Hirokawa, K. (1975) X-ray photoelectron spectroscopy of Co₃O₄, Fe₃O₄, Mn₃O₄ and related compounds. Journal Electron Spectroscopy and Related Phenomena, 7, 405–473.

Oku, M., Hirokawa, K., and Ikeda, S. (1975) X-ray photoelectron spectroscopy of manganese-oxygen systems. Journal Electron Spectroscopy and Related Phenomena, 7, 465–473.

Polissar, M.J. (1935) The kinetics of the reaction between permanganate and manganous ions. Journal of Physical Chemistry, 39, 1057–1066.

Pratt, A.R., McIntyre, N.S., and Splinter, S.J. (1998) Deconvolution of pyrite, marcasite and arsenopyrite XPS spectra using the maximum entropy method. Surface Science (in press).

Pratt, A.R., Muir, I.J., and Nesbitt, H.W. (1994) X-ray photoelectron and Auger electron spectroscopic studies of pyrrhotite and mechanism of air oxidation. Geochimica Cosmochimica Acta, 59, 1773–1786.

Purcell, K.F. and Kotz, J.C. (1977) Inorganic Chemistry, 1116 p. Saunders, Pennsylvania.

Rao, C.N.R., Sarma, D.D., Vasudevan, S., and Gegde, M.S. (1979) Study of transition metal oxides by photoelectron spectroscopy. Proceedings of the Royal Society of London, A 367, 239–262.

Scott, M.J. and Morgan, J.J. (1995) Reactions at oxide surfaces: 1. Oxidation of As(III) by synthetic birnessite. Enironmental Science and Technology, 29, 1898–1905.

Shannon, R.D. (1976) Revised effective ionic radii and systematic studies of interatomic distances in halides and chalcogenides. Acta Crystallographica, A32, 751–767.

Sheppard, J.C. and Wahl, A.C. (1957) Kinetics of the manganate-permanganate exchange reaction. Journal of the American Chemical Society, 70, 1020–1024.

Stumm, W. and Morgan, J.J. (1981) Aquatic Chemistry, 583 p. Wiley, New York.

Tanuma, S., Powell, C.J. and Penn, D.R. (1991) Calculations of electron inelastic mean free paths: III. Surface and Interfacial Analysis, 17, 927–939.

Vasquez, R.P., Klein, J.P., Barton, J.J., and Grunthaner, F.J. (1981) Application of maximum-entropy spectral estimation to deconvolution of XPS data. Journal Electron Spectroscopy, 23, 63–81.

APPENDIX
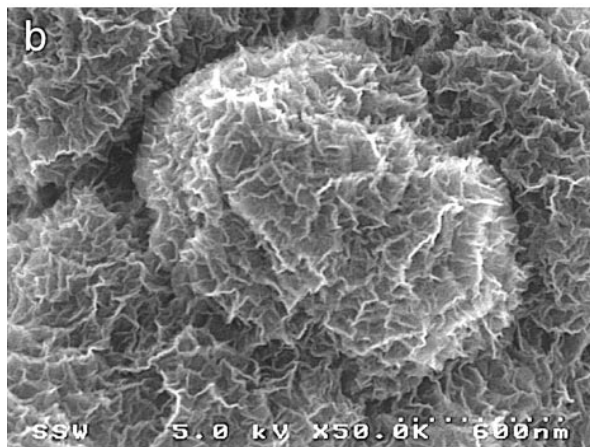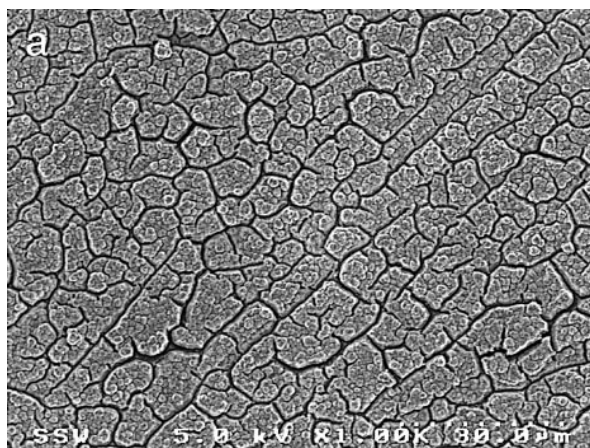
(**a**) SEM images of a thickened synthetic birnessite coating on an aluminum disk. (**b**) High magnification of a portion of the thickened coating illustrating the texture and surface morphology of the coating. The morphology indicates the presence of only one phase.